CST 2010

The 26th Conference of the Mechanical Engineering Network of Thailand
October 2012, Chiang Rai

Finite Element Modeling of Creasing in Corrugated Paperboards

Anucha Saysroy, Petch Jearranaisilawong*

Department of Mechanical and Aerospace Engineering,
King Mongkut's University of Technology North Bangkok,
1518 Pibulsongkram Rd. Bangsue, Bangkok 10800.
*Corresponding Author: petchj@kmutnb.ac.th, 08-9813-1519.

Abstract

The purpose of this study is to understand mechanical response of corrugated paperboards under creasing process. Paperboards are composite materials consisting of layers of corrugating medium, each sandwiched between a pair of liners. In the manufacturing process, a pattern of crease (or score) lines are pressed onto the surface of paperboards to facilitate folding and bending. Yet, over-pressing of the crease lines can cause cracks on the liners or severe deformation of the corrugating medium, while under-pressing can lead to insufficient depth for folding. To determine an optimal creasing depth for folding, the mechanics of creasing was analyzed in a set of numerical simulations using a commercial finite element software ABAQUS. Geometrical features of paperboards, such as liners and medium were modeled in details. Each layer of paper was modeled by an orthotropic elasto-plastic material with a plastic potential whose parameters were obtained from relevant experiments. The analysis focuses on mechanics of creasing at three distinct positions on the fluting pattern of corrugating medium. Creasing between two peaks of the fluting produces the highest tensile stress, which leads to permanent damage along the crease line on the top liner. On the other hand, applying a creasing pattern on top of the peaks of fluting leads to buckling of the corrugating medium. The proposed simulations shred lights into the mechanics of crease line that can be used for improving crease pattern and for reducing cracks along the creasing line in the manufacturing process.

Keywords: Creasing, Corrugated Paperboards, Finite element

1. Introduction

Corrugated paperboard is a composite sandwiched structure of paper sheets. Its construction consists of corrugated sheets termed flute, core, or medium glued between two layers of outer flat sheets termed linerboards or liners. An example of components of a single wall corrugated paperboard is shown in Fig. 1-1.

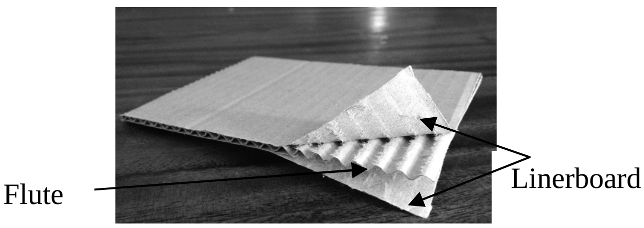

Fig. 1-1 Components of corrugated paper.

Corrugated paperboard is produced in a two-step process: the wet process is where the medium sheet is corrugated between two rolls and glued onto the liners, and the dry process is the application of heat onto the corrugated paperboard to dry and remove excessive moisture. A schematic of manufacturing process of corrugated board is illustrated in Fig. 1-2.

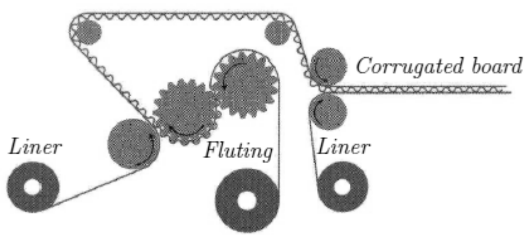

Fig. 1-2 Manufacturing process of corrugated paperboard [1].

Corrugated paperboard are folded along pre-pressed or 'crease' lines to form three dimensional structures. Crease lines affect two attribute of paperboards: they enhance bending stiffness along the crease lines, which is important for load carrying capacity of paperboard structure, but reduce bending stiffness transverse to the crease lines, which facilitate folding process. In the past, attempts have been made to predict the load-carrying capacity of corrugated paperboard boxes by McKee [5]. More recent work addressing this problem can be found in Nordstrand [6], who investigated post buckling strength of corrugated paperboard panels and boxes. Biancolini et al. [3] developed a finite element simulation framework to gain a better understanding of how a corrugated board panel deforms under mechanical loads. They suggested that during the box manufacturing process the corrugated board may be severely deformed, particularly in the folded areas. Yet, they did not produce a conclusive analysis of the strength of paperboard along the folded lines. This work intends to address the strength along the folded area by simulating the creasing process of corrugated paperboard panel and then using the developed framework for strength analysis of the folded paperboard structure. Simulations in this report are limited to a single-wall paperboard which has two liners and a corrugating medium. Further, a representative corrugated paperboard selected in this study is a symmetric board, which indicates the same type of paper for top and bottom liners.

2. Mechanical behavior and material properties of a sheet of paper

A sheet of paper is an orthotropic material that exhibits mechanical response with three principal directions due to preferential alignments of constituent fibers. The in-plane direction along the paper roll is machine direction (MD), the other in-plane direction perpendicular to MD is cross machine direction (CD) and the out-of-plane direction is thickness direction (ZD). Fig. 2-1 shows the material directions in a sheet of paper. Following the manufacturing process, the mechanical response of corrugated paperboard also exhibits three principal directions that are co-aligned with those of sheet of paper.

Mechanical response of a thin sheet of paper is modeled by a shell structure where the in-plane response dominates that of the out-of-plane direction. The in-plane response is investigated by means of uniaxial tensile tests along the MD and CD. Typical in-plane stress-strain curves in MD and CD are demonstrated in Fig. 2-2. The MD has a higher axial modulus and stress at failure than those along the CD. On the other hand, along the CD a sheet of paper can undergo a larger maximum strain. Linearity at the beginning of the two stress-strain curves is observable, and may be treated as elastic behavior describable by a set of orthotropic elastic moduli. Following the linear parts, the stress-strain curve becomes nonlinear with decreasing tangent moduli. The onsets of nonlinearity can be treated as yield points. Following the classical theory of plasticity, the stress-strain curves can be decomposed into an elastic part and a plastic part ($\varepsilon = \varepsilon^e + \varepsilon^p$). The development of plastic strain and an increase in the yield stress (σ_y) are equivalent to hardening law in the classical theory. Therefore, the paper sheet is constitutively modeled as an orthotropic elasto-plastic material with orthotropic hardening, which in ABAQUS corresponds to an orthotropic elastic lamina with an orthotropic plastic potential.

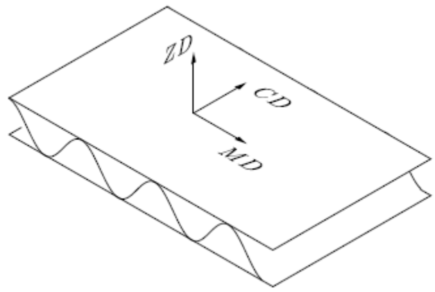

Fig. 2-1 Material directions in a sheet of paper

The required material parameters needed to calibrate the constitutive model for the nonlinear FE simulation of sheets of paper were obtained from uniaxial tensile tests. Tensile specimens were straight coupons of 15 mm width and 180 mm length. Tests were categorized into four groups: liner along MD, liners along CD, corrugated medium along MD, and corrugated medium along CD. Fig. 2-2 and 2-3 illustrate the measured stress–strain relationship of the liner and medium specimens under both MD and CD. For simple representation, MD is denoted by 1-direction, CD by the 2-direction and ZD by the 3-direction here in.

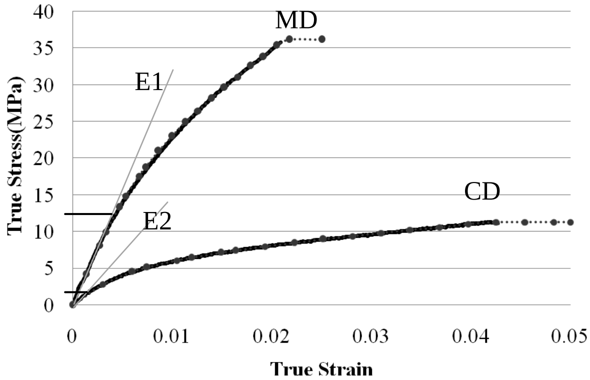

Fig. 2-2 Stress–strain relationship of linerboard, solid line is experiment and dot line is simulation.

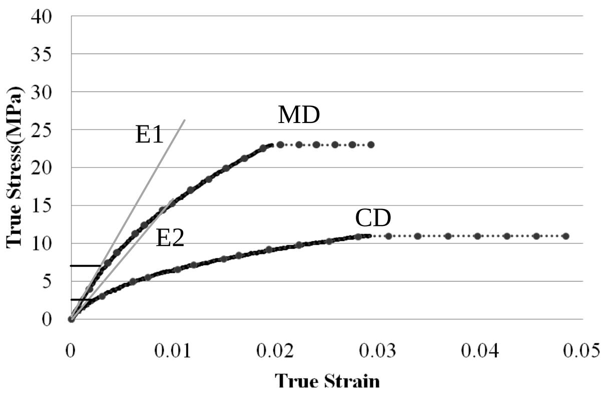

Fig. 2-3 Stress–strain relationship of medium, solid line is experiment and dot line is simulation.

Table. 2-1 shows elastic moduli and Poisson's ratios of the liner and medium. The in-plane elastic moduli were obtained from the experiments. Poisson's ratios used in the simulations follow Nordstrand [6], $\nu_{12} = 0.34$ and $\nu_{13} = \nu_{23} = 0.01$. Shear moduli G_{12}, G_{13}, and G_{23} were calculated from the axial moduli using the relationships by Baum [2];

$$G_{12} = 0.387\sqrt{E_1 E_2}\,, G_{13} = E_1/55, G_{23} = E_2/35 \quad (1)$$

Table. 2-1 Elastic material properties of linerboard and medium

Properties	Liner	Medium
E_1 (MPa)	3149.47	2203.04
E_2 (MPa)	1075.36	1133.95
ν_{12}	0.34	0.34
G_{12} (MPa)	712.21	611.67
G_{13} (MPa)	89.98	62.94
G_{23} (MPa)	19.55	20.62

The orthotropic plastic potential defined in ABAQUS, a standard constitutive model for sheet metals, will be adapted to model orthotropic plastic hardening behavior. The model parameters include a base yield curve and a set of weighting parameters, R_{11}, R_{22}, R_{33}, R_{12}, R_{13}, and R_{23} representing anisotropic yield stress ratios with respect to the base curve along each principal and shear directions. The stress ratios are defined in Eq. 2

$$R_{11} = \frac{\bar{\sigma}_{11}}{\sigma^0}, R_{22} = \frac{\bar{\sigma}_{22}}{\sigma^0}, R_{33} = \frac{\bar{\sigma}_{33}}{\sigma^0}, \quad (2)$$
$$R_{12} = \frac{\bar{\sigma}_{12}}{\tau^0}, R_{13} = \frac{\bar{\sigma}_{13}}{\tau^0}, R_{23} = \frac{\bar{\sigma}_{23}}{\tau^0}$$

where $\bar{\sigma}_{11}$ is initial yield stress in MD
$\bar{\sigma}_{22}$ is initial yield stress in CD
$\bar{\sigma}_{33}$ is initial yield stress in ZD
$\bar{\sigma}_{12}$ is shear stress in MD-CD
$\bar{\sigma}_{13}$ is shear stress in MD-ZD
$\bar{\sigma}_{23}$ is shear stress in CD-ZD
σ_0 is reference yield stress
τ_0 is reference shear stress, $\tau^0 = \sigma^0/\sqrt{3}$

In this work, the base plastic curve is that of the CD, $\bar{\sigma}_{22} = \sigma_0$ and hence, $R_{22} = 1$. Further, the out-of-plane direction as denoted by 3-direction is assumed to be equivalent to the 2-direction. Note that ABAQUS models out-of-plane stiffness as purely elastic for shell formulation, and the out-of-plane assumption is irrelevant to the results. Calculated stress ratios are shown in Table 2-2.

Table. 2-2 Orthotropic stress ratios.

	R_{11}	R_{22}	R_{12}
Liner	3.2	1	2.1
Medium	2.1	1	1.55

3. Creasing simulation of corrugated paperboard

A corrugated paperboard was constructed by connecting peaks of fluting of corrugating medium to top and bottom liners at the contact nodes. Thus, the interfaces between each layer are assumed to be rigidly connected. Corrugating pattern of the medium layer was geometrically modeled in details following measured dimensions from a micrograph of cross section of the paperboard, see Fig. 3-1. Simulated paperboard is a square board of 100-by-100 mm^2, and the thickness of the paperboard is defined by the height of corrugating medium. A sheet thickness of 0.18274 mm was used for all layers. Individual paper sheets are meshed by 4-node quadratic shell with reduced integration element (S4R). The creaser is modeled as a rigid body with dimensions in Fig. 3-2.

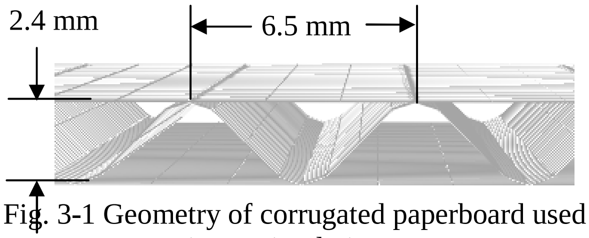

Fig. 3-1 Geometry of corrugated paperboard used in FE simulations.

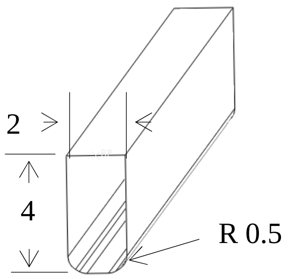

Fig. 3-2 Geometry of creaser.

Creasing of corrugated paperboard was directed at three positions relative to peaks of fluting in the corrugating medium:
position I is at the peak of a fluting,
position II is between a peak and a valley, and
position III is located at the middle between two peaks. Fig. 3-3 illustrates the described creasing positions.

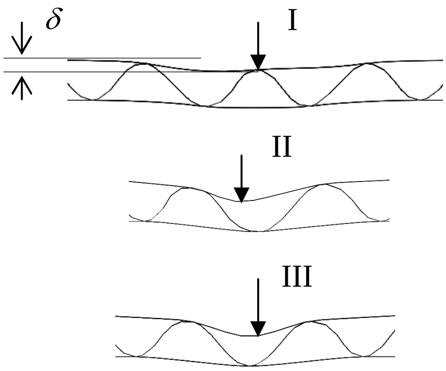

Fig. 3-3 Creasing of corrugated board at three positions.

Creasing is simulated by lowering the creaser to a specified creasing depth on the corrugated paperboard with fixed bottom liners. Loading and boundary conditions used in the simulations are shown in Fig. 3-4.

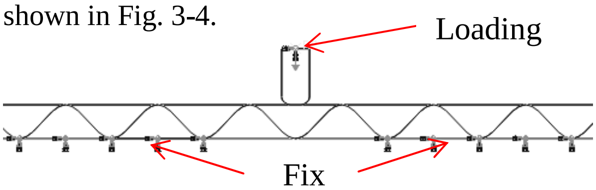

Fig. 3-4 Loading and boundary conditions.

Results of the simulations are plotted in terms of reaction force at the creaser and the creasing depth in Fig. 3-5.

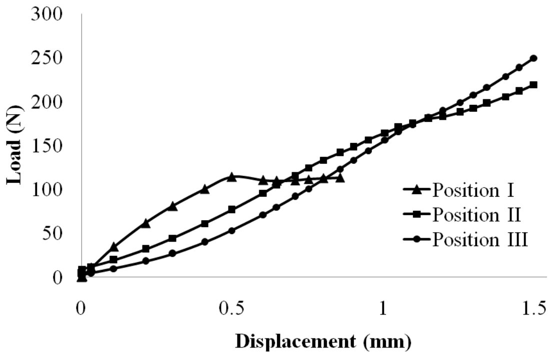

Fig. 3-5 Load-Displacement curve of creasing at three positions.

Creasing at position I exhibits a stiffer response compared to the other two positions. The response of the structure when creased at position I exhibits an initial stiff force-displacement response that reaches a plateau at a depth of 0.50 mm, which corresponds to buckling of the corrugating medium. On the other hand, the response at position III is approximately linear; its dominating mechanism is stretching of the top liner. The response at position II reflects a combined responses of I and III where the response is first dominated by stretching of the top liner followed by buckling of the corrugating medium at the critical depth of 1.1 mm. Creasing causes breakage of liners along the crease line. In the simulations, damage corresponds to a tensile stress of each layer exceeding the limiting stress of the paper sheet. The simulation results show that for creasing at position I the maximum tensile stresses occur at the flute area whereas the damages for position III and II are found on the top liner. In addition, the plot of maximum tensile stresses and creasing depth of each creasing position in Fig. 3-6 shows that the damage occurs at position III at the smallest creasing depth, and the damage at position I and II happen at the same creasing depth. In another word, the top liner is more susceptible to damage from crease than the corrugating medium.

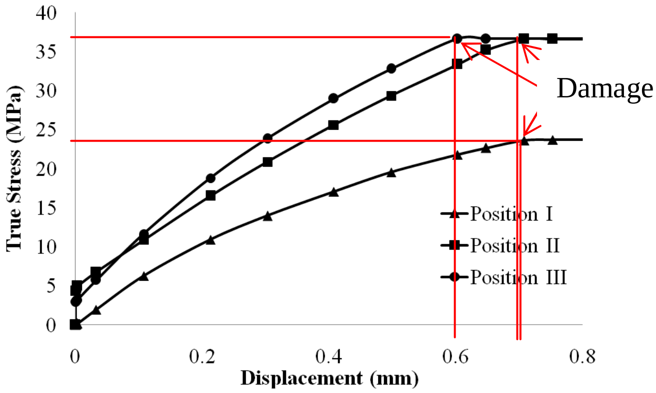

Fig. 3-6 Stress-Displacement curve of creasing at three positions.

4. Conclusions

This report demonstrates two aspects of simulations of corrugated paperboard. First the mechanical response of a sheet of paper can be constitutively modeled by an orthotropic elastic-plastic material using the plastic potential as a yield surface and hardening parameters. Second, the simulation of creasing process of corrugated paperboard reveals that the damage due to creasing likely will occur due to tensile breakage of the liners.

5. References

[1] A. Allansson, (2001). Stability and collapse of corrugated board ; Numerical and Experimental Analysis, *Structural Mechanics LTH, Sweden.*

[2] Baum, G.A., Brennan, D.C. and Habeger, C.C, (1981) Orthotropic elastic constants of paper, *Tappi*, Vol. 64, No. 8, pp 97-101.

[3] Biancolini, M.E., Brutti, C., (2005). Evaluation of equivalent stiffness properties of corrugated board, *Composite Structure*, No. 69, pp 322–328.

[4] Harrysson, A., Ristinmaa, M., (2008). Large strain elasto-plastic model of paper and corrugated board, *International Journal of Solids and Structures*, No. 45, pp. 3334–3352.

[5] McKee C, Gander JW, Wachuta JR., (1963). Compression strength formula for corrugated boxes, *Paperboard Packaging*, No. 40, pp.149–159.

[6] Nordstrand, T.M., (1995). Parametric study of the post-buckling strength of structural core sandwich panels, *Composite Structures*, Vol. 30, pp 441- 451.